Dynamics of basal lamina fenestrations in the rat intestinal villous epithelium in response to dietary conditions

Rie Azumi[1, 2], Keisuke Morita[2], Yusuke Mizutani[2], Manabu Hayatsu[2], Shuji Terai[1], and Tatsuo Ushiki[2]

[1]Division of Gastroenterology, Niigata University Graduate School of Medical and Dental Sciences, Niigata, Japan

[2]Division of Microscopic Anatomy, Niigata University Graduate School of Medical and Dental Sciences, Niigata, Japan

Address correspondence to: Prof. Tatsuo Ushiki, Division of Microscopic Anatomy, Niigata University Graduate School of Medical and Dental Sciences, Asahimachi-dori 1, Chuo-ku, Niigata 951-8510, Japan

Tel: +81-25-227-2062, Fax: +81-25-224-1767

E-mail: t-ushiki@med.niigata-u.ac.jp

ABSTRACT

The epithelial basal lamina of the small intestine forms a felt-like sheet at the base of the epithelium. Previous studies have shown that the basal lamina has numerous fenestrations, which are produced by leucocytes penetrating through the basal lamina. In this study, we aimed to directly visualize fenestrations of the rat basal lamina in intestinal villi by scanning electron microscopy (SEM) after removal of the villous epithelium by osmium maceration and ultrasonic treatment. Structural changes in fenestrations were then investigated in relation to dietary conditions. SEM of these tissues revealed the presence of fenestrations in the villous epithelial basal lamina in all segments of the small intestine, although the number was the highest in the jejunum. The present study also showed that the number and size of fenestrations increased after feeding in the jejunum, whereas changes were unclear in the ileum. These findings suggested that the basal lamina fenestrations were changed through the dynamics of migrating leucocytes in dietary conditions and may also be related to the regulation of nutrient absorption, particularly as lipids are transported from the intercellular space of the epithelium to the lamina propria.

INTRODUCTION

The small intestine has numerous small finger-like or foliated projections in its luminal surface, which are referred to as intestinal villi. These villi are covered with epithelial tissue, which absorbs nutrients and provides a barrier against harmful substances. Transmission electron microscopy (TEM) has shown that the intestinal epithelium consists of a single layer of columnar epithelial cells on top of a continuous sheet of basal lamina (16). Because epithelial cells are sealed by the zonula occludens on the apical side, large nutrients, including carbohydrates and proteins, are absorbed from the intestinal lumen into the epithelial cells after digestion to smaller molecules (e.g., monosaccharides and amino acids); these smaller molecules are then released from the basolateral side of the cells, followed by accumulation in the blood capillary network beneath the epithelium (12). Neutral fats are also absorbed from the apical membrane of epithelial cells as monoglycerides and fatty acids, which are resynthesized into triacylglycerol in epithelial cells and released from the basolateral side of the cells as chylomicrons (2). These chylomicrons then enter the connective tissue of the lamina propria and are finally collected into lacteals or lymphatic capillaries (11).

Free cells, such as lymphocytes, eosinophils, and macrophages, often migrate into the epithelium, as demonstrated by light microscopy and TEM (4, 10, 15, 17).

Migration of these intraepithelial leukocytes is accompanied by the formation of fenestrations in the epithelial basal lamina, and these structures have been observed by scanning electron microscopy (SEM) (8, 6, 13, 14). Interestingly, some investigators have also shown that chylomicrons pass though these fenestrations because chylomicron particles are too large (roughly 100 nm to 1 μm in diameter) to pass through the basal lamina if there are no interruptions (11). These findings suggest that fenestrations in the epithelial basal lamina may be related to leukocyte migration and may play an important role in nutrient uptake (particularly chylomicron uptake) in the intestinal villus.

Thus, the aim of the present study was to investigate the role of basal lamina fenestrations in response to dietary conditions. For this purpose, we observed fenestrations in the rat basal lamina of intestinal villi by SEM after removal of the villous epithelium by osmium maceration and ultrasonic treatment. Structural changes in the fenestrations were then investigated under fasted and fed states. The results suggested that the size and number of basal lamina fenestrations were changed depending on the dietary condition and these changes may affect nutrient conditions, particularly lipid absorption.

MATERIALS AND METHODS

This study was carried out in accordance with the Niigata University Animal Experimental Guidelines after approval by the Ethics Committee for Niigata University Animal Experimentation (No. 340-2).

Animals. Male Wistar rats (Japan SLC, Inc. Shizuoka, Japan), 8–10 weeks old, were used in this study. The rats were divided into two groups, each of which consisted of three animals. The animals in the first group were fasted for 22 h, whereas those in the second group were fasted for 22 h and then fed pellets (Rodent Lab Diet EQ; PMI Nutrition International Inc., Brentwood, MO, USA) for 2 h. Animals in both groups were anesthetized by intraperitoneal injection of pentobarbital sodium and then perfused through the heart with physiological saline followed by 4% paraformaldehyde (0.1 M phosphate buffer).

Light microscopy. After perfusion fixation, the middle jejunum was excised, immersed in the same fixative (4% paraformaldehyde) overnight, embedded in paraffin, and cut to a thickness of 5 μm. The sections were stained with hematoxylin and eosin (HE), and observed with an optical microscope (ECLIPSE E 600; Nikon, Tokyo, Japan).

TEM. The upper jejunum was excised from the perfusion-fixed body, cut into small pieces, and fixed by immersion in 2% glutaraldehyde (0.1 M phosphate buffer) for 4 h.

Samples were further fixed with 1% osmium tetroxide for 1 h, dehydrated with a graded ethanol series, and embedded in epoxy resin. Ultrathin sections (60–80 nm thickness) were prepared using an ultramicrotome, stained with uranyl acetate and lead citrate, and observed with a transmission electron microscope (H-7650; Hitachi, Tokyo, Japan).

SEM analysis of osmium-macerated/ultrasonicated tissues. Segments of the upper jejunum, middle jejunum, lower jejunum, and middle ileum were removed from the perfusion-fixed body and immersed in 2% glutaraldehyde (0.1 M phosphate buffer) for 2 days. Transverse slices of each intestinal segment, at a thickness of 300 μm, were prepared using a microslicer (DTK-1000; Dosaka EM). The sections were then immersed in a 2% osmium tetroxide aqueous solution for 3 days in a thermostatic chamber (20°C) for tissue maceration and further treated in an ultrasonic bath (Bransonic Ultrasonic Cleaner; Branson Ultrasonics, Emerson Japan, Atsugi, Japan) for 10–20 min to completely remove the epithelium from the intestinal villi. The samples were then stained with 1% tannic acid solution for 2 h and 1% osmium tetroxide for 2 h, dehydrated in a graded ethanol series (70%, 80%, 90%, and 95% for 30 min each and 100% for 30 min three times), and dried in a critical point dryer (CPD-2; Hitachi). The dried samples were mounted on aluminum stubs with double-sided carbon tape, coated with platinum-palladium using a magnetron sputtering coater (MSP-10;

Vacuum Device Co. Ltd., Ibaraki, Japan), and observed using a scanning electron microscope (S-3700; Hitachi) at an accelerating voltage of 7 or 20 kV. In this study, backscattered electron (BSE) images were obtained with a highly sensitive, annular BSE detector.

Statistical analysis. SEM images of the villus associated with complete removal of epithelial covering were used for statistical analysis. Because rat intestinal villi are foliate in shape, each SEM image of a single villus was carefully captured at an accelerating voltage of 7 kV after the flat surface was positioned horizontally with respect to the imaging surface. The number and area of fenestrations as well as the area of the epithelial basal lamina were then measured from these SEM images using ImageJ software. Briefly, a dark area showing a roundness of 0.4–1 with a size of 15 pixels (real area: 0.59 μm^2) or more, was recognized as a fenestration in the villus and was automatically marked with red color. We then carefully judged the results and checked for fenestrations that could not be automatically captured because of bending or folding of the villus; these were manually marked in red using image processing software (Photoshop CS 5; Adobe Systems Inc., CA, USA). Fenestrations associated with the free cells in the lower layer were also colored green. Finally, free cells just passing through fenestrations were marked with blue dots.

The output data were transferred to Excel to calculate the total number and area of fenestrations for each villus. The number of fenestrations per unit area of the villus, the area of each fenestration, and the number of free cells in each villus were also compared in different segments of the small intestine between the fasting group and feeding-after-fasting group. In order to avoid preparation artifacts (e.g., shrinkage or distortion of the villus), we calculated the number and area of fenestrations in the middle 60% of the entire height of each villus. The level of significance was defined as 0.05.

RESULTS

Light microscopy and transmission electron microscopy

Light microscopy of HE-stained sections revealed the basic structure of the villus in the jejunum (Fig. 1a, b). Free cells, such as eosinophils and lymphocytes, were often observed in the villous epithelium of all animals investigated in this study. The number of intraepithelial leukocytes tended to be greater in the feeding-after-fasting group than in the fasting group, but it was difficult to accurately evaluate the difference between the two groups. There were also leukocytes passing through the epithelial basement membrane, suggesting the presence of fenestrations in the basement membrane,

although they could not be visualized by light microscopy.

TEM analysis showed that free cells could be observed between the epithelial cells just above the basal lamina (Fig. 1c). These intraepithelial cells were identified mainly as eosinophils and granular lymphocytes, some of which were in the process of passing through the epithelial basal lamina (Fig. 1d, e). There were also interruptions in the epithelial basal lamina without leukocytes.

SEM

The villous epithelial cells were almost completely removed from the specimen after osmium maceration and ultrasonic treatment, which enabled direct SEM observation of the entire surface of the villous basal lamina. These SEM images clearly showed that the villous basal lamina had numerous fenestrations.

Basic structure of the epithelial basal lamina of the intestinal villus. BSE imaging with an accelerating voltage of 20 kV is useful for visualizing subsurface structures because BSE signals at higher accelerating voltages can produce “see through” images of samples. Using this technique, the blood capillary network beneath the epithelial basal lamina was clearly observed in relation to the localization of basal lamina fenestrations (Fig. 2a). At higher magnification, fenestrations were found to be located in the region free from the lower capillary network, but not in the region facing the capillaries

themselves (Fig. 2b). The fenestrations were oval or round in shape and ranged from 0.5 to 6 μm in diameter. Fenestrations with migrating leukocytes were also found.

SEM observations of different segments of the small intestine showed that the height of the intestinal villi was greatest in the upper jejunum and decreased as the intestine reached the ileum (Fig. 3a–d). Thus, the area of the villi was also the greatest in the upper jejunum and the smallest in the ileum (Table in Fig. 3), suggesting that the absorption efficiency was different in the various segments of the small intestine, with the highest absorption observed in the upper part of the jejunum.

Statistical analysis of basal lamina fenestrations

For statistical analysis, we used BSE images at an accelerating voltage of 7 kV because the fenestrations were dark enough to be analyzed using ImageJ software at this voltage (Fig. 4). For each micrograph, fenestrations without free cells were colored red, those associated with free cells were colored green, and free cells passing through fenestrations were indicated by blue dots (Fig. 4). Calculation of the number and size of fenestrations was made at the central region (60%) of villi, as described in Materials and Methods.

The number of fenestrations in the fasting group was highest in the upper jejunum and decreased toward the lower jejunum, but increased in the ileum.

Statistically, the number of fenestrations was significantly larger in the upper jejunum than in the lower jejunum ($p = 0.005$; Fig. 5).

Comparison of basal lamina fenestrations between the fasting and feeding-after-fasting groups. The number of fenestrations per unit area was used for comparison between the two groups because the sizes of individual villi were not the same. Our results showed that the number of fenestrations per unit area tended to increase in the feeding-after-fasting group, although a significant difference was found only in the lower jejunum ($p = 0.02$) (Fig. 6).

The sizes of fenestrations were also compared between the two groups by calculating the average area of each villus (Fig. 7). The area of the fenestrations was greater in the upper jejunum than in the lower jejunum in both groups, but there were no significant difference between the two groups. However, the histogram created using the number and area of fenestrations revealed that small fenestrations (less than 1.5 μm^2) decreased and large fenestrations (more than 6 um^2) increased in the upper and middle jejunum (and ileum) in the feeding-after-fasting group (Fig. 8).

Figure 9 shows the average values and standard deviations of the area of fenestrations per unit area in each segment of the two groups. The area of fenestrations was significantly greater in the feeding-after-fasting group than in the fasting group.

These quantitative and statistical findings suggested that migrating cells were more active in the upper jejunum than in the lower jejunum and that the sizes of basal lamina fenestrations increased due to leukocyte migration through the fenestrations in response to dietary conditions.

Fenestrations with migrating leukocytes. The number of migrating leukocytes passing through fenestrations was compared between the two groups (Fig. 10). The number of leukocytes was significantly greater in the upper jejunum of the feeding-after-fasting group than in the fasting group, suggesting that migrating leukocytes increased in the upper jejunum in response to feeding.

DISCUSSION

In this study, we investigated the structures of basal lamina fenestrations in the rat intestinal villi and showed changes in the size and number of fenestrations in response to dietary conditions. The presence of basal lamina fenestrations has been visualized by SEM using either osmium maceration or boric acid treatment (6, 8, 13, 14). Here, we also showed that osmium maceration plus ultrasonic treatment was useful for the complete removal of villous epithelial cells, thus enabling direct observation of the intestinal basal lamina by SEM.

With regard to the distribution of basal lamina fenestrations, Komuro (6) reported that fenestrations were mostly present in the upper two-thirds of the villi, except for the extreme top, and Takeuchi and Gonda (14) also showed that the fenestrations were mainly distributed in the upper three-fourths of the villi. We confirmed these previous findings and demonstrated the presence of regional differences in the number of fenestrations from the upper jejunum to the ileum.

We also clarified that the size of the villi was greatest in the upper jejunum and decreased as the small intestine reached the ileum.

In this study, changes in the size and number of basal lamina fenestrations were evaluated for the fasting and feeding-after-fasting groups. Our findings showed that some fenestrations were increased in the feeding-after-fasting group, suggesting that migration of free cells became active in the jejunum (particularly in the upper jejunum) in response to feeding. We also showed that these migrating leukocytes were mainly composed of eosinophils and granular lymphocytes.

The reason for the high migrating activity of leukocytes in the jejunum in response to feeding is unclear. Some investigators have demonstrated the presence of nutrient-induced inflammation in the intestine (5). This inflammation is thought to be produced by stimulation of intestinal immune cells (including macrophages and

intraepithelial lymphocytes) and epithelial cells to release cytokines through fat absorption (3, 9). Eosinophils are often found in the villous epithelium and the lamina propria and are thought to play a role in the maintenance of the normal immune environment (1). Although the mechanism of leukocyte activation is complicated and unclear, it is probable that activation induces an increase in leukocyte migration into and/or from the intestinal epithelium, resulting in enlargement of basal lamina fenestrations during nutrient absorption in the intestinal villi.

In contrast, previous investigators have demonstrated that chylomicrons are released into the lateral wall of absorptive epithelial cells and accumulated in the space between the absorptive cells delineated by the epithelial basal lamina (11). They also noticed the presence of breaks in the basal lamina, which may facilitate the movement of chylomicrons from the intercellular space to the lamina propria. These basal lamina breaks recognized by TEM are apparently basal lamina fenestrations, which can be directly observed by SEM of macerated tissues. Because the fenestrations were present in the mesh of the lower capillary network, they also acted as a functional route, connecting the intercellular space to the free space of the lamina propria.

Taken together, our findings suggested that the basal lamina formed a barrier between the intercellular space and the lamina propria and that the basal lamina

fenestrations of the intestinal villi provided important pathways for large nutrients, such as chylomicrons, to be released from the epithelial side to the space of the lamina propria. In this context, increased fenestration size may be functionally important for facilitating fat absorption during feeding.

Previous studies have shown that fat absorption is completed mainly in the jejunum (7). The activation of free cells in the jejunum revealed in the present study may also support the concept that basal lamina fenestrations are related to lipid absorption. In order to confirm this, we are currently investigating the dynamics of basal lamina fenestrations in response to a fatty diet.

In conclusion, we investigated the structures of epithelial basal lamina fenestrations in the rat intestinal villi and demonstrated that the size and number of fenestrations increased in the jejunum after feeding. From these findings, we suggested that the basal lamina fenestrations were changed through the dynamics of migrating leukocytes in dietary conditions, and may also be related to the regulation of nutrient absorption, particularly as the lipids are transported though these fenestrations from the intercellular space of the epithelium to the lamina propria.

REFERENCES

1. Bowcutt R, Forman R, Glymenaki M, Carding SR, Else KJ and Cruickshank SM (2014) Heterogeneity across the murine small and large intestine. *World J Gasteroenterol* **20**, 15216-15232.

2. Green PHR and Glickman RM (1981) Intestinal lipoprotein metabolism. *J Lipid Res* **22**, 1153-1173.

3. Hara Y, Miura S, Komoto S, Inamura T, Koseki S, Watanabe C, Hokari R, Tsuzuki Y, Ogino T, Nagata H, Hachimura S, Kaminogawa S and Ishii H (2003) Exposure to fatty acids modulates interferon production by intraepithelial lymphocytes. *Immunol Lett* **86**,139-148.

4. Ishikawa H, Naito T, Iwanaga T, Takahashi-Iwanaga H, Suematsu M, Hibi T and Nanno M (2007) *Curriculum vitae* of intestinal intraepithelial T cells: their developmental and behavioral characteristics. *Immunol Rev* **215**, 154-165.

5. Ji Y, Sakata Y and Tso P (2011) Nutrient-induced inflammation in the intestine. *Curr Opin Clin Nutr Metab Care* **14**, 315-321.

6. Komuro T (1985) Fenestrations of the basal lamina of intestinal villi of the rat. Scanning and transmission electron microscopy. *Cell Tissue Res* **239**, 183-188.

7. Kawano S, Sanada Y, Chiba M, Nakagami T and Toki A (2010) Effect of fat supplementation on the maintenance of gut integrity in elemental diet-fed rats. *Eur*

J Pediatr Surg **20**, 399-404.

8. McClugage SG and Low FN (1984) Microdissection by ultrasonication: porosity of the intestinal epithelial basal lamina. *Am J Anat* **171**, 207-216.
9. Miura S, Tsuzuki Y, Hokari R and Ishii H (1998) Modulation of intestinal immune system by dietary fat intake: relevance to Crohn's disease. *J Gastroenterol Hepatol* **13**, 1183-1190.
10. Palay SL and Karlin LJ (1959) An electron microscopic study of the intestinal villus. I. The fasting animal. *J Biochem Cytol* **5**, 363-371.
11. Patrick T and Balint JA (1986) Formation and transport of chylomicrons by enterocytes to the lymphatics. *Am J Physiol* **250**, G715-G726.
12. Shimizu M (2010) Interaction between food substances and the intestinal epithelium. *Biosc Biotechnol Biochem* **74**, 232-241.
13. Takahashi-Iwanaga H, Iwanaga T and Isayama H (1999) Porosity of the epithelial basement membrane as an indicator of macrophage-enterocyte interaction in the intestinal mucosa. *Arch Histol Cytol* **62**, 471-481.
14. Takeuchi T and Gonda T (2004) Distribution of the pores of epithelial basement membrane in the rat small intestine. *J Vet Med Sci* **66**, 695-700.
15. Toner PG and Ferguson A (1971) Intraepithelial cells in the human intestinal

mucosa. *J Ultrastr Res* **34**, 329-344.

16. Yamamoto T (1982) Ultrastructural basis of intestinal absorption. *Arch Histol Jpn* **45**, 1-22.

17. Yantiss RK (2015) Eosinophils in the GI tract: how many is too many and what do they mean? *Modern Pathol* **28**, S7-S21.

Figure legends

Fig. 1. Light micrographs (a, b) and transmission electron micrographs (c–e) of the villus in the rat middle jejunum. **a.** Villi from the fasting group. Arrowheads indicate intraepithelial leukocytes. La: lacteal. **b.** Villi from the feeding-after-fasting group. Several leukocytes (arrowheads) were also observed in the epithelium. The arrow indicates a leukocyte passing through the basement membrane. **c.** TEM image of a part of the villus in the jejunum of the feeding-after-fasting group. White arrows indicate the epithelial basal lamina. L: intraepithelial lymphocyte. **d.** TEM image of a lymphocyte (L) passing through a fenestration in the basal lamina (arrow). **e.** An eosinophil (E) passing through the basal lamina (arrow). Scale bar: 2 μm (c), 1 μm (d, e).

Fig. 2. Scanning electron micrographs of the intestinal villus treated with osmium maceration and ultrasonication in the rat middle jejunum of the feedind-after-fasting group. These images were obtained in BSE mode at an accelerating voltage of 20 kV for producing "see-through" images. **a.** Intestinal villus shape. Blood capillaries beneath the basal lamina were clearly observed as a network of cord-like structures. **b.** High magnification of the image shown in b. All fenestrations were located in the portion in which lower capillaries were absent. The fenestrations ranged in size from 0.5–6 μm in diameter. The arrow indicates a leukocyte passing through the fenestration.

Fig. 3. Intestinal villi from the different segments of the small intestine (fasting group) after removal of epithelial cells by osmium maceration/ultrasonication (**a.** upper jejunum, **b.** middle jejunum, **c.** lower jejunum, and **d.** ileum). Villi showed a leaf-like shape, but the height was greatest in the upper jejunum and decreased toward the ileum. **Table**. The average area of the villi for the different segments of the small intestine.

Fig. 4. SEM images of the intestinal villi found in the upper jejunum of the feeding-after-fasting group. For statistical analysis, BSE images at an accelerating voltage of 7 kV (**a**) were used because fenestrations were observed as dark spots compared with the bright surface of the basal lamina. In the right micrograph (**b**), fenestrations without free cells are colored red, and those associated with free cells are colored green. Free cells passing through fenestrations are also indicated as blue dots. Calculations were made in the middle 60% of the entire height of each villus (framed by the yellow line).

Fig. 5. Number of fenestrations per villus in the fasting group.

Fig. 6. The average number of fenestrations per villous area in the fasting and feeding-after-fasting groups.

Fig. 7. The area of a single fenestration in different segments of the small intestine in fasting and feeding-after-fasting groups.

Fig. 8. Histograms of the number and area of fenestrations in the fasting (white) and feeding-after-fasting (red) groups. **a.** Upper jejunum, **b.** middle jejunum, **c.** lower jejunum, **d.** ileum.

Fig. 9. The area of fenestrations per unit area. The area of fenestrations tended to increase in all segments in the feeding-after-fasting group compared with that in the fasting group, although the increase was not statistically significant, except in the upper jejunum.

Fig. 10. The number of free cells passing through fenestrations, and the number of cells per total number of fenestrations in different segments of the small intestine in the fasting and feeding-after-fasting groups.

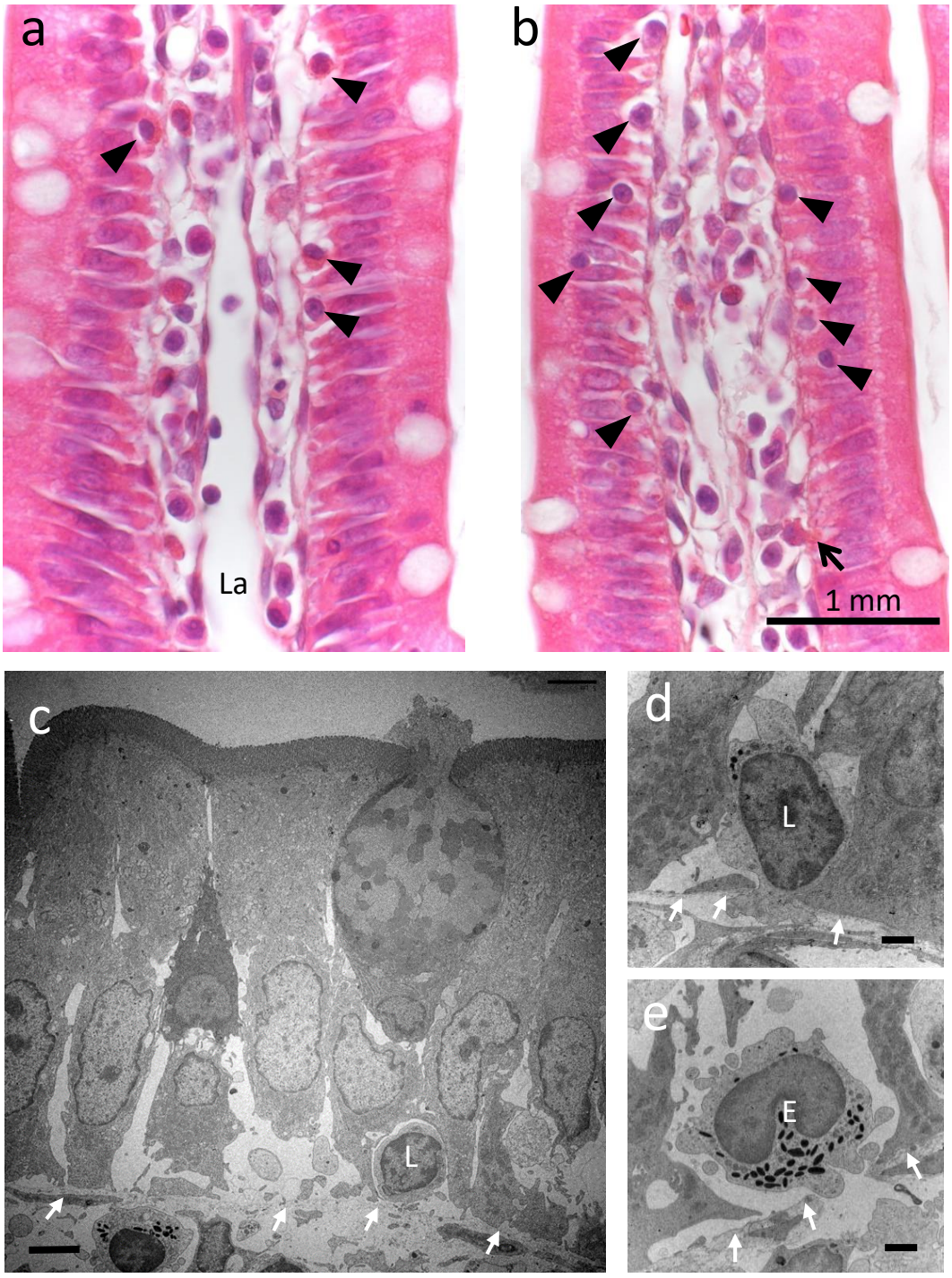

Fig. 1

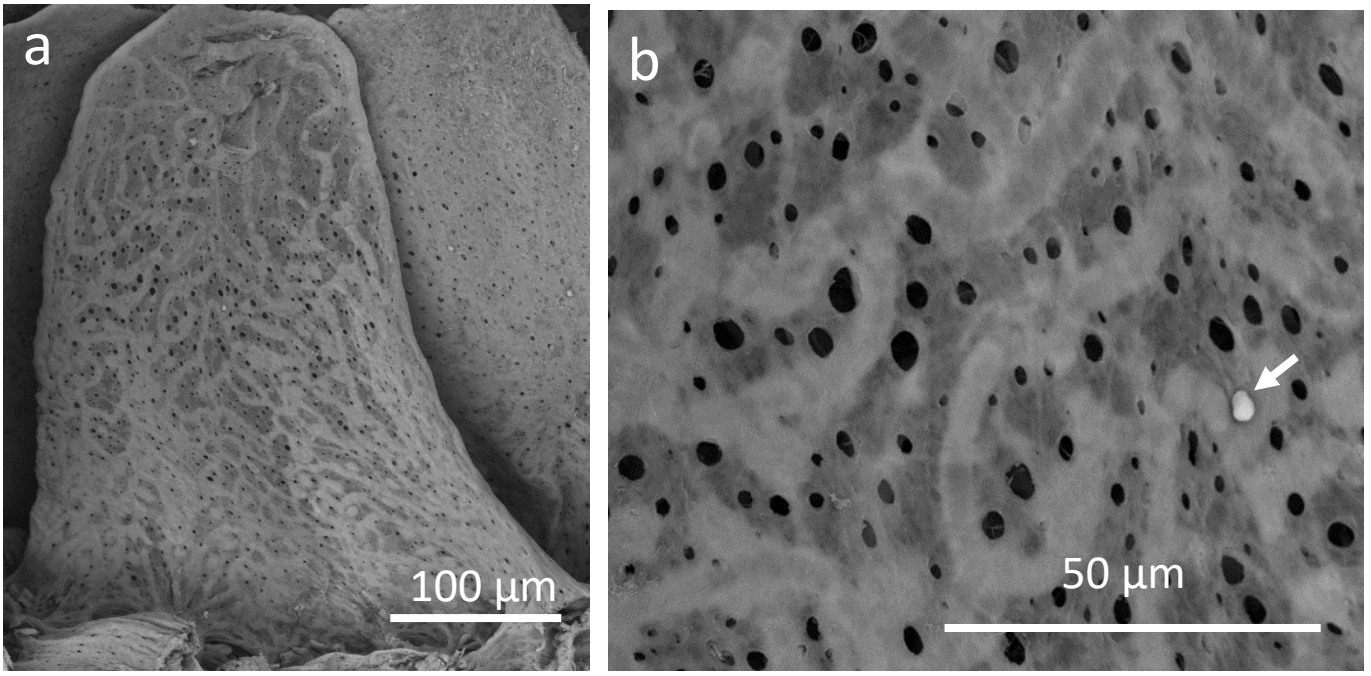

Fig. 2

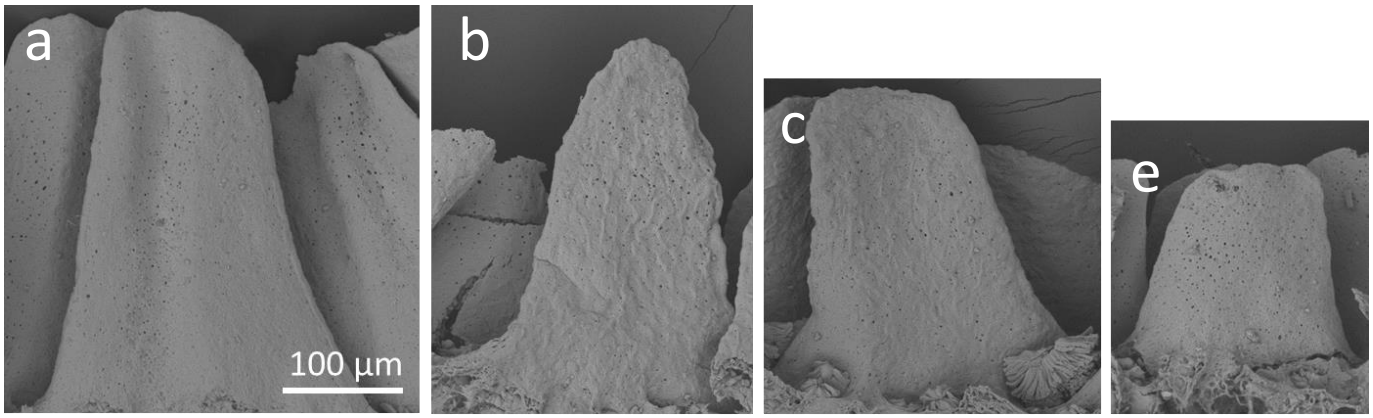

upper jejunum middle jejunum lower jejunum ileum

upper jejunum		middle jejunum		lower jejunum		ileum	
average	S.D.	average	S.D.	average	S.D.	average	S.D.
5.00	1.20	4.62	1.23	3.52	1.08	3.23	0.73

area of a single villus x $10^4 \mu m^2$

Fig. 3

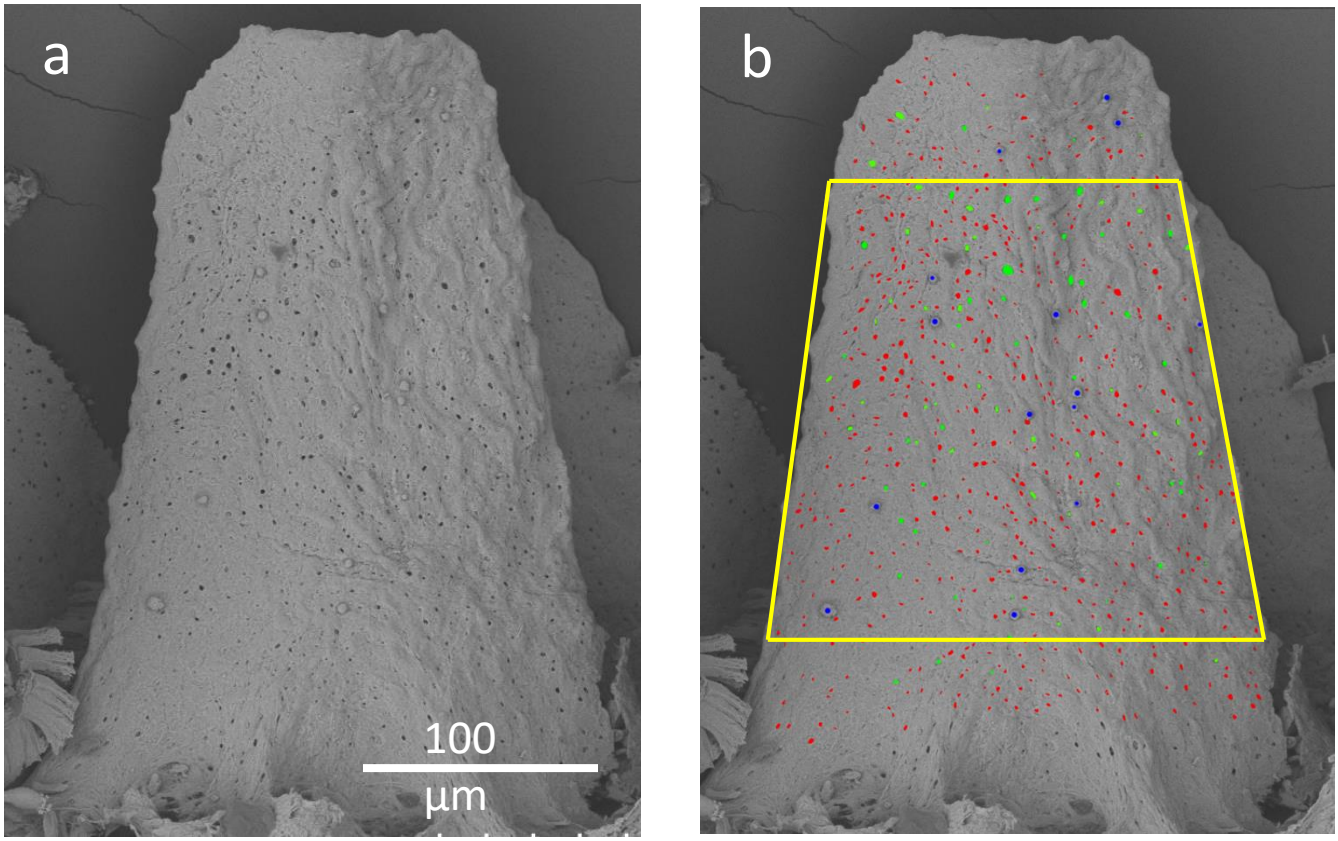

Fig. 4

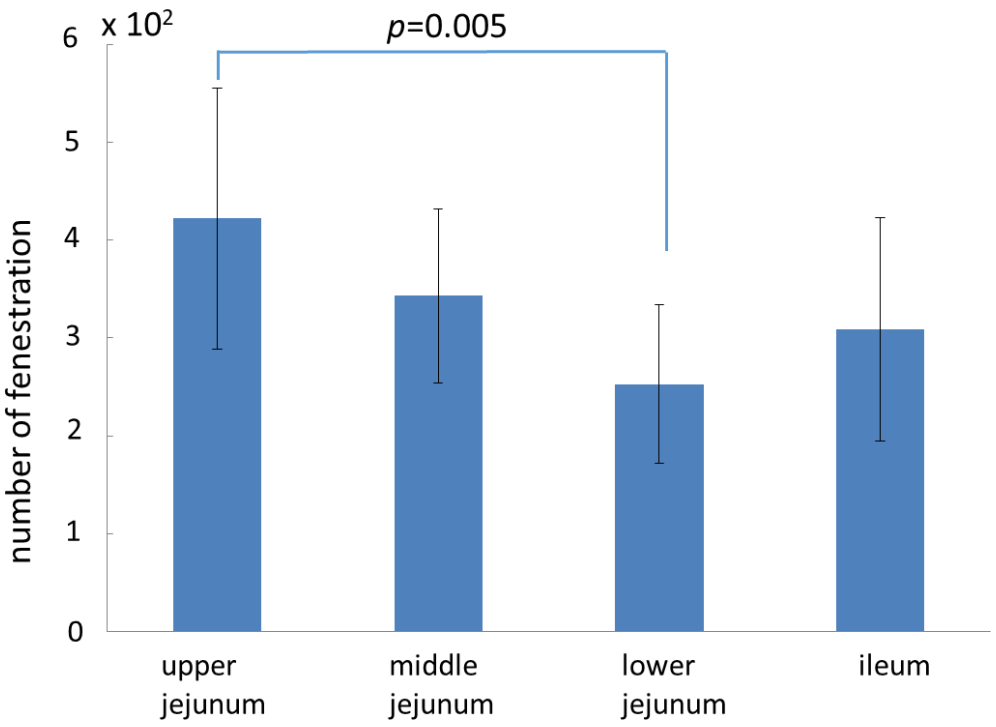

upper jejunum		middle jejunum		lower jejunum		ileum	
average	S.D.	average	S.D.	average	S.D.	average	S.D.
4.22	1.33	3.43	0.89	2.53	0.81	3.09	1.14

number of fenestrations/villi (60%) x 10^2

Fig. 5

	upper jejunum		middle jejunum		lower jejunum		ileum	
	average	S.D.	average	S.D.	average	S.D.	average	S.D.
fasting	1.35	0.184	1.21	0.22	1.16	0.26	1.58	0.27
feeding-after-fasting	1.49	0.31	1.31	0.31	1.42	0.26	1.73	0.27
t-test	0.10		0.42		0.02		0.21	

Number of fenestration /area of a single villus x 10^2 /μm^2

Fig. 6

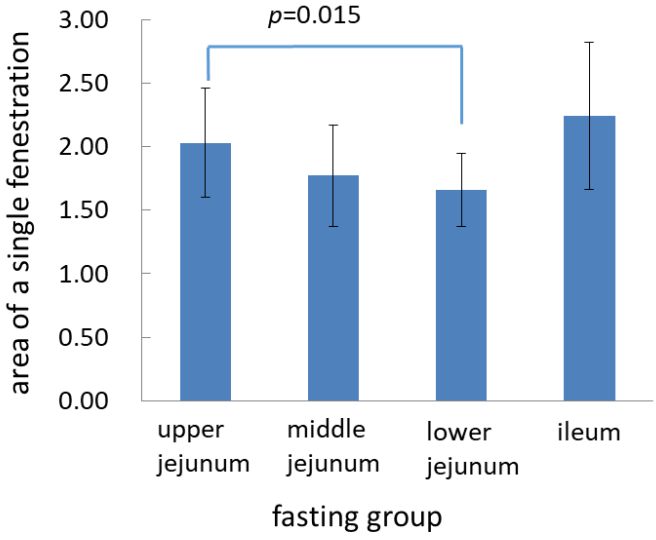

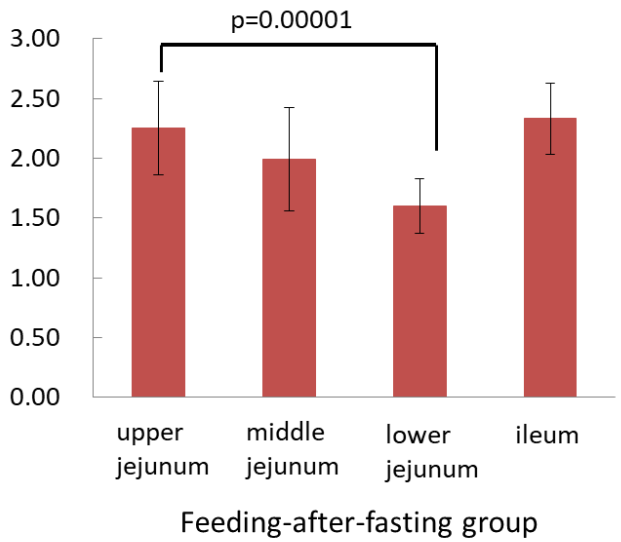

	upper jejunum		middle jejunum		Lower jejunum		ileum	
	average	S.D.	average	S.D.	average	S.D.	average	S.D.
fasting	2.03	0.43	1.77	0.40	1.66	0.29	2.24	0.58
feeding-after-fasting	2.25	0.39	1.99	0.43	1.60	0.23	2.33	0.30

μm^2

Fig. 7

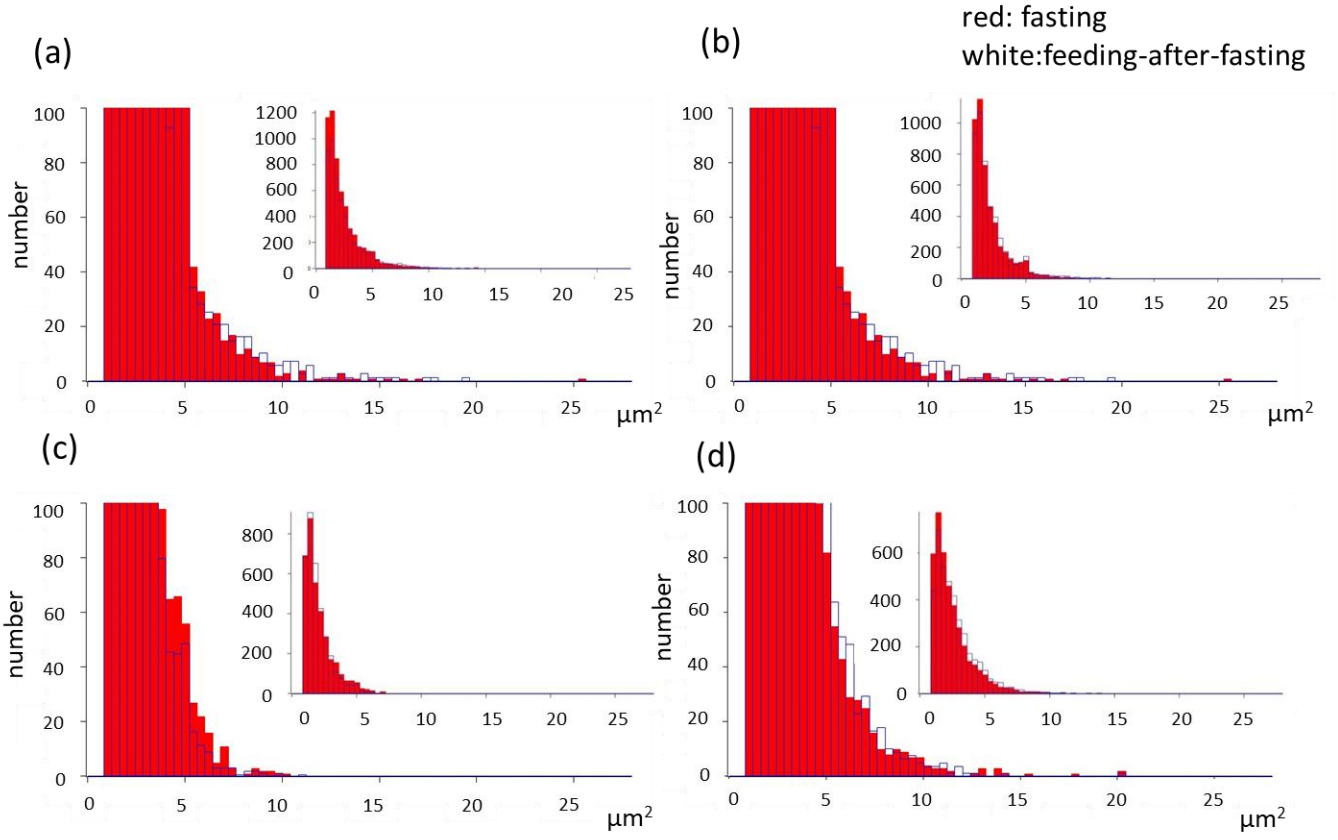

Fig. 8

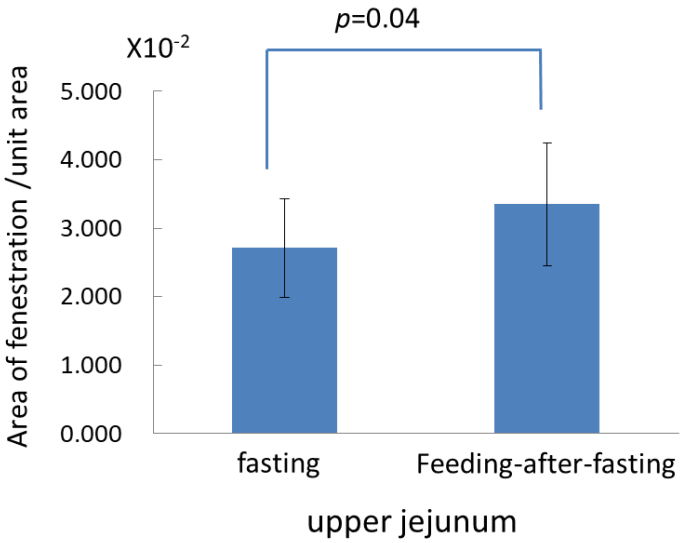

	upper jejunum		middle jejunum		lower jejunum		ileum	
	average	S.D.	average	S.D.	average	S.D.	average	S.D.
fasting	2.71	0.72	2.12	0.45	1.96	0.65	3.75	0.94
feeding-after-fasting	3.35	0.90	2.70	1.25	2.22	0.48	4.05	0.60
t-test	0.04		0.21		0.22		0.38	

x 10^{-2}

Fig. 9

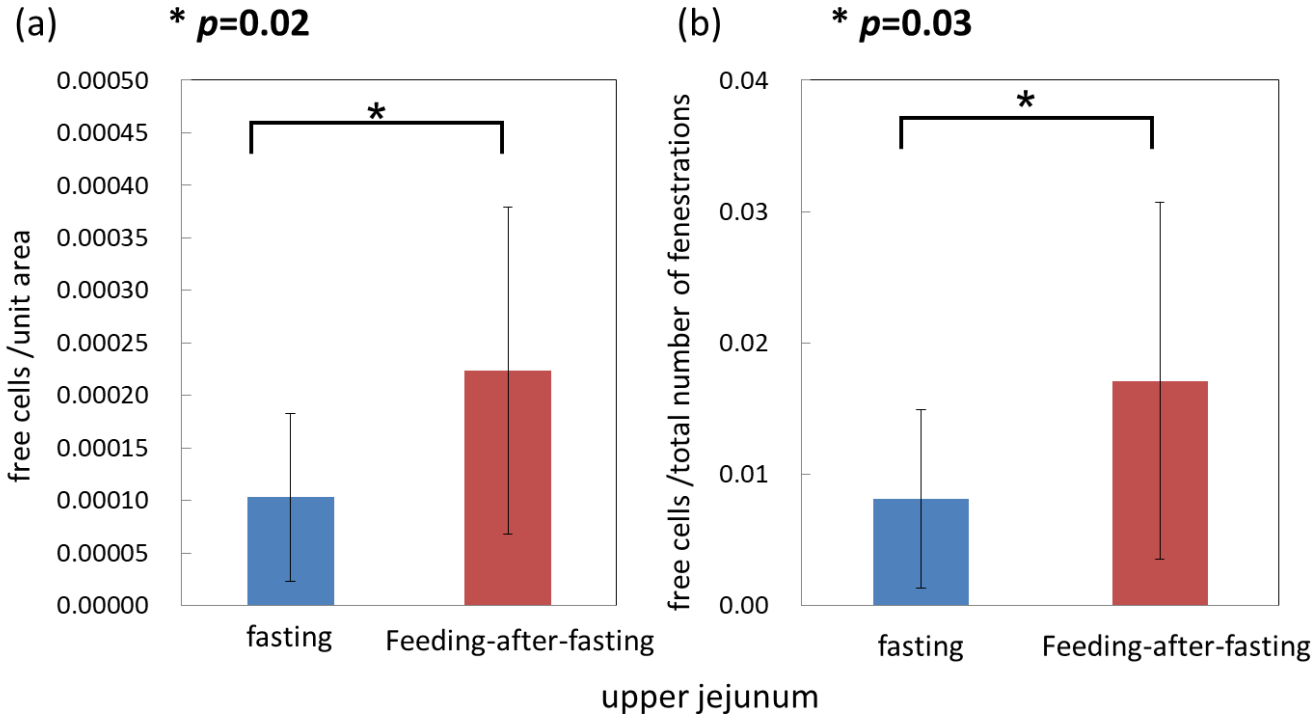

upper jejunum

	upper jejunum		middle jejunum		lower jejunum		ileum	
	average	S.D.	average	S.D.	average	S.D.	average	S.D.
fasting	0.10	0.08	0.33	0.29	0.22	0.11	0.17	0.15
feeding-after-fasting	0.22	0.16	0.32	0.21	0.17	0.13	0.17	0.13
t-test	0.02		0.87		0.13		0.92	

number of free cells x 10^{-3} /μm^2

	upper jejunum		middle jejunum		lower jejunum		ileum	
	average	S.D.	average	S.D.	average	S.D.	average	S.D.
fasting	0.81	0.68	2.77	0.26	2.05	1.16	0.98	0.77
feeding-after-fasting	1.71	1.36	2.67	1.92	1.44	1.31	0.94	0.76
t-test	0.03		0.91		0.09		0.89	

free cells /total number of fenestrations x 10^{-2}

Fig. 10